September 2, 2020

2019 International Conference on Indoor Positioning and Indoor Navigation (IPIN), 30 Sept. - 3 Oct. 2019, Pisa, Italy

State Observability through Prior Knowledge: Tracking Track Cyclers with Inertial Sensors

1st Tom L. Koller
Multi-Sensoric Interactive Systems
University of Bremen
Bremen, Germany
tkoller@uni-bremen.de

2nd Udo Frese
Multi-Sensoric Interactive Systems
University of Bremen
Bremen, Germany
ufrese@uni-bremen.de

***Abstract*—Inertial Navigation Systems suffer from unbounded errors on the position and orientation estimate. This drift can be corrected by applying prior knowledge, instead of using exteroceptive sensors. Analysing the state observability induced by prior knowledge motivates us to track bikers in track cycling races. In this paper, we show that the pose of the bikers can be estimated with an IMU as the only sensor by using a heightmap of the track and the knowledge that the biker drives forward. We present a dataset with three 60-round trials and evaluate the state estimate. We show that the influences of the priors match the expectation derived from state observability analysis.**

***Index Terms*—State Estimation, Prior Knowledge, Inertial Navigation System, INS, Track Cycling**

I. Introduction

For short time periods, the pose (position and orientation) of an object can be estimated with an Inertial Measurement Unit (IMU). The pose is estimated by integrating the acceleration and angular rate measurements. This method accumulates the measurement errors of the IMU, wherefore the estimate drifts over time. The drift can be corrected by fusing the IMU with exteroceptive sensors, e.g. GPS.

In indoor environments, GPS is unavailable. Custom radio emitters or the buildings WiFi can be used instead [1]. Surprisingly, several pedestrian tracking systems achieve drift-free estimates with an IMU alone [2]–[4]. The systems fuse IMU measurements with prior knowledge of the environment and the motion dynamics, instead of using an additional sensor.

Fusing IMU measurements with prior knowledge is a powerful concept to gain drift-free estimates [5]. The knowledge allows to observe otherwise unobservable states. These approaches have the advantage that they do not require additional sensor hardware in the buildings. Furthermore, most users already carry the necessary IMU in their smartphone [2].

With a smartphone IMU, pedestrians can be localized with accuracies of 1.3 m [6]. The common approach for pedestrian tracking [2] is to detect the moment of the human gait cycle, where the foot stands still on the ground. A Zero-Velocity Update (ZUPT) is applied to correct the velocity drift [7]. Then, the position estimate is refined by mapping motions [2] and activities [6] to building plans in a Particle Filter (PF) .

DFG-Funding: ZaVI FR 2620/3-1

Fig. 1. The track of the Sixdays Bremen

We investigate how knowledge affects the observability of states. We will analyse the state observability independently of applications, but we will try to bridge the gap between theory and application. As a whole, we want to elevate the fusion of knowledge and IMU measurements to a paradigm of state observability through prior knowledge. In our position paper [5], we argued that the prior knowledge that is available for track cycling is sufficient to track a track cycler with an IMU as the only sensor. Now, we develop a state estimator for track cycling and confirm our conjecture with an experiment.

Tracking track cyclers is motivated by prior knowledge used in the literature. The forward velocity prior for wheeled vehicles [8] has a similar effect as the ZUPT. It states that a wheeled vehicle has approximately zero velocity perpendicular to its forward direction. The prior allows to observe the forward velocity from IMU measurements if the vehicle is driving a curve. Additionally, IMU biases are observable [9]. Since the bike track contains two 180° curves (see Fig. 1), the velocity and biases get occasionally observable with the prior.

Several works use a map to improve the state estimate. The map can have different forms, e.g. route maps [10]–[12] with the paths that can be taken or building plans [3] with impassable walls. With a terrain map, a vehicle can be localized without a GPS [13]. At track cycling, the bikers are constrained to stay on the track (see Fig. 1), which can be modelled as a height- or terrain map.

Intuitively, we argue that the heightmap corrects the global position drift. The global drift is a result of the accumulation of small sensor errors. The forward velocity prior reduces the global drift, but does not correct it. The prior improves the accuracy of local segments so that curves and straights can be distinguished. The knowledge that the bike stays on the track forces the state estimator to align the local segments with the heightmap. This should correct the forward drift except for the track's symmetry.

In the curve, the velocity is observable and the angular rate is measured. Hence, we can estimate the curve radius of the track cycler. The curve radius depends on the lateral position of the biker on the track. Therefore, the lateral position can be determined in the curves.

We present a state estimator that uses the shown prior knowledge to track the pose of a track cycler. The state estimation is formulated as a least squares optimization problem and solved with ceres [14]. We show the capability of the state estimator on a track cycling dataset with three 60-round trials. We also present methods based on prior knowledge to retrieve an initial guess for the optimizer and to handle missing IMU measurements. We will evaluate the influence of the used knowledges on the quality of the state estimate.

The remainder of the paper is structured as follows. Section II shows how to model the prior knowledge to use it in the least squares state estimator. We show methods to derive an initial guess and to handle missing data based on prior knowledge and give practical implementation details in Section III. In Section IV, the dataset is described. Our results are shown and evaluated in Section V. Finally, we will sum up the results in the conclusion.

II. Knowledge based Optimization problem

At track cycling, bikers race on a track. There are several game modes with varying strategies [15]. In our setup, the bikes are equipped with wireless IMUs as shown in Fig. 2.

The trajectory is estimated by finding the trajectory with the maximum a-posteriori probability given the measurements of the Main frame IMU, the dynamic model and the prior knowledge. We formulate the state estimation as a minimization problem and solve it by using the ceres least squares solver [14]. The solver works offline and optimizes the whole problem at once.

The state estimation can be seen as a sequence of n states x_k, $0 < k <= n$ (see Fig. 3) connected by the dynamic model:

$$x_{k+1} = g_k(x_k) \tag{1}$$

Instead of using the input for the dynamic update, the state does contain every information needed for the dynamic model.

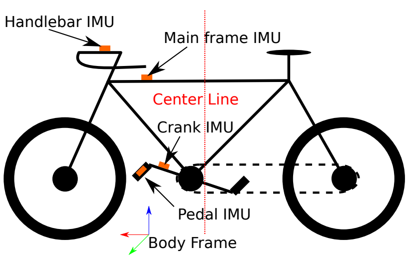

Fig. 2. Bike with IMUs. Only the main frame IMU is used.

The inputs are used as a constraint on the respective state. The prior knowledge constrains every state of the trial.

Each state x_k consists of the position $\vec{p}_W$, velocity $\vec{v}_W$ and acceleration $\vec{a}_W$ in world frame; the rotation from body to world Q_W^B, the angular rate $\vec{\omega}_B$ and acceleration $\vec{\omega}'_B$; and the biases of the accelerometer $\vec{b}_a = \vec{b}_{a1} + \vec{b}_{a2}$ and the gyrometer $\vec{b}_g = \vec{b}_{g1} + \vec{b}_{g2}$. The components always refer to x_k, wherefore we can omit the k-indices for readability:

$$x_k = \begin{pmatrix} \vec{p}_W & \vec{v}_W & \vec{a}_W & Q_W^B & \vec{\omega}_B & \vec{\omega}'_B & \vec{b}_a & \vec{b}_g \end{pmatrix}^T \tag{2}$$

The orientation Q_W^B is modelled as an Euler-Rodriguez rotation matrix. Usually, the acceleration and angular rate are modelled as inputs instead of states. We chose to add them to the state to apply prior knowledge on them. Furthermore, we defined the point on the ground under the Main frame IMU as the body frame (see Fig. 2), instead of the IMU pose, because the chosen prior knowledge does not hold for the IMU pose.

The complete parameter space X of the optimization problem consists of the states at all steps:

$$X = \{x_1, \cdots, x_n\} \tag{3}$$

We want to find the most likely sequence of states given the inputs $\vec{ac}_k$ and $\vec{gy}_k$, the input functions $a_k(x_k)$ and $\omega_k(x_k)$, the dynamic model $g_k(x_k)$ and our prior knowledges, i.e. the heightmap $h_k(x_k)$ and the forward velocity prior $fv_k(x_k)$. This can be calculated by solving the minimization problem (4) at the top of the next page, where $||v - \hat{v}||^2_\Sigma$ is the Mahalanobis distance. The $\boxminus$ is a normal minus operation, despite that - for rotation matrices - it returns the difference as a rotation vector, i.e. an unit-axis scaled by an angle [16]:

$$x^* \boxminus x = \{\vec{p}^*_W - \vec{p}_W, \overbrace{\cdots, \log({Q_W^B}^T Q_W^{B*})}, \vec{\omega}^*_B - \vec{\omega}_B, \cdots\} \tag{5}$$

Its purpose is to handle the manifold structure of Q_W^B.

The minimization problem is formulated by simply adding up information about the states. The first information added is the gyrometer input at each time step. Each state has to match the measured angular rate. With $\omega_k(x_k)$, we calculate a prediction of the angular rate and compare it with the measurement. By imposing the difference of the prediction and the measurement as an error, the optimizer will adapt each

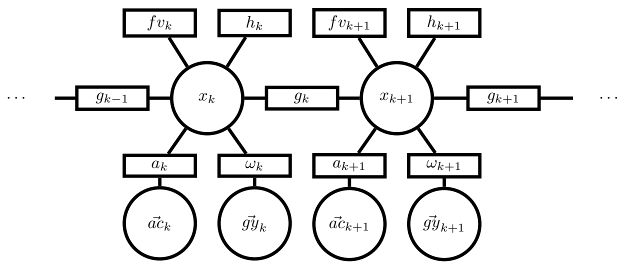

Fig. 3. The optimization problem as FactorGraph. $\vec{ac}_k$ and $\vec{gy}_k$ are the inputs, x_k is the state, g_k the dynamic model (8), a_k the acceleration function (7), ω_k the angular rate function (6), and fv_k the forward velocity prior (9) and h_k the heightmap prior (10).

$$\hat{X} = \arg\min_{X} \sum_{k=1}^{n} \left[\underbrace{||\omega_k(x_k) - \vec{gy}_k||^2_{\Sigma_{gy}}}_{\text{gyrometer input}} + \underbrace{||a_k(x_k) - \vec{ac}_k||^2_{\Sigma_{ac}}}_{\text{accelerometer input}} + \underbrace{||g_k(x_k) \boxminus x_{k+1}||^2_{\Sigma_g}}_{\text{dynamic model}} + \underbrace{||fv_k(x_k)||^2_{\Sigma_{fv}}}_{\text{forward velocity prior}} + \underbrace{||h_k(x_k)||^2_{\Sigma_h}}_{\text{heightmap prior}} \right] \quad (4)$$

state x_k until the prediction and the measurement coincide. This is similar to the measurement step in a Kalman Filter.

The prediction of the angular rate can be calculated by:

$$\omega_k(x_k) = Q_I^B * \vec{\omega}_B + \vec{b}_g \quad (6)$$

where the calibrated rotation matrix Q_I^B transforms $\vec{\omega}_B$ from body to IMU frame. The $*$ denotes matrix multiplication.

The second information that we have about the states is the accelerometer input. Similar to the gyrometer input, the predicted accelerations $a_k(x_k)$ and the acceleration measurements $\vec{ac}_k$ have to match. Since the IMU is not at the origin of the body frame, the IMU measures accelerations induced by rotational movements. Additionally, the acceleration in the state is gravity free. Those accelerations are taken into account by the prediction function:

$$\begin{aligned} a_k(x_k) = {} & Q_I^B * (Q_W^B)^T * (\vec{a}_W - \vec{g}_W) \\ & + Q_I^B * ([\vec{\omega}'_B]_\times + [\vec{\omega}_B]^2_\times) * \vec{t}_I + \vec{b}_a \end{aligned} \quad (7)$$

where $\vec{g}_W$ is the gravity vector and $[\cdots]_\times$ forms a skew symmetric matrix out of the given vector. $\vec{t}_I$ is the calibrated offset between IMU and body frame.

The dynamic model $g_k(x_k)$ connects the states x_k and x_{k+1} over time. The predicted next state $g_k(x_k)$ has to match the next state x_{k+1}. The dynamic model is based on the classic Inertial Navigation System (INS) state space model [17, Sec. 3.7.1]:

$$g_k(x_k) = \begin{pmatrix} \vec{p}_W + \Delta t \cdot \vec{v}_W + \frac{\Delta t^2}{2} \cdot \vec{a}_W \\ \vec{v}_w + \Delta t \cdot \vec{a}_W \\ \vec{a}_W \\ Q_W^B * \exp(\Delta t \cdot \vec{\omega}_B) \\ \vec{\omega}_B + \Delta t \cdot \vec{\omega}'_B \\ \vec{\omega}'_B \\ \vec{b}_{a1} \cdot (1 - \frac{\Delta t}{T_{cor1}}) \\ \vec{b}_{a2} \cdot (1 - \frac{\Delta t}{T_{cor2}}) \\ \vec{b}_{g1} \\ \vec{b}_{g2} \cdot (1 - \frac{\Delta t}{T_{cor3}}) \end{pmatrix} \quad (8)$$

$$T_{cor1} = 1000, \qquad T_{cor2} = T_{cor3} = 2000$$

where Δt is the time difference. The accelerometer bias is modelled as the sum of two exponential auto correlated random walk functions with decorrelation constants T_{cor1} and T_{cor2}. The gyrometer bias is modelled as the sum of a constant and an exponential auto correlated random walk function with decorrelation constant T_{cor3}. $\exp(\cdots)$ is the Euler-Rodriguez Formula [16]. Cartesian and angular acceleration stay constant in the dynamic model, but do not contribute to the error calculation. Thus, they can change arbitrary between states.

In contrast to the other information, the prior knowledges are shown without a target value to compare. However, prior knowledge often has a target value which is either constant or state dependent itself. For example, the forward velocity prior can be formulated as [8]:

$$fv_k(x_k) = (Q_W^B)^T * \vec{v}_W - \begin{pmatrix} * \\ 0 \\ 0 \end{pmatrix} \quad (9)$$

where the target for the y- and z-dimension of the body velocity is 0. The asterisk is a wildcard, which allows arbitrary velocity in forward direction. If a measurement of the x-dimension is available, e.g. by odometry, it can be used instead. In our model, the x dimension is unused.

The heightmap prior states that the wheels of the bike stay at the track. We approximate this by constraining the body frame, which is between the wheels, to stay on the track. This means that the distance between the position $\vec{p}_W$ and the closest point on the track has to be 0, or otherwise stated:

$$h_k(x_k) = \vec{p}_W - \arg\min_{\vec{c}_W \in Track} ||\vec{p}_W - \vec{c}_W|| \quad (10)$$

where $Track$ is the set of all points on the track. In this case, the prediction $\vec{p}_W$ is trivial but the target value is state dependent.

In this manner, additional information can be added simply by adding it to (4). The optimizer will incorporate it weighted by the covariance of the knowledge.

The covariances are crucial tuning parameters of the model. Neither the forward velocity prior, nor the heightmap prior hold exactly. Side slip can occur, which results in a side velocity. The heightmap itself is imperfect. Furthermore, the bike may bounce on surface irregularities. Those imprecisions of the knowledge are modelled in the covariance of the measurement equations. If the knowledge is violated more than expected, the estimator's performance will be reduced.

III. Implementation

The modelled problem in (4) can be solved with any least squares solver. In this chapter, we will show what we have done technically to get a converging solution.

A. The initial guess

The convergence of a least squares solver depends on the initial guess of the states. Especially in the presence of state dependent constraints, the solver may stay in unsuitable local minima. We designed a method based on prior knowledge to provide an initial guess for the least squares solver. This method is again based on another, but more simple model.

The initial guess method exploits the basic form of the track. In principle, the track consists of two straight lines connected with two curves (see Fig. 4). As a vague model of the track, we

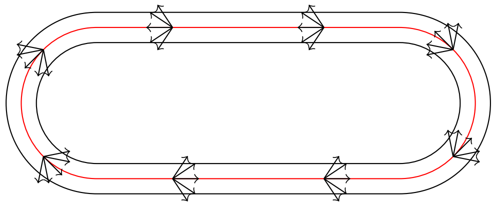

Fig. 4. Basic form of the track. The red line shows the 1D simplification. The arrows show the possible heading range.

assume that the bikers follow the 1D line. This model requires big noise in lateral direction and for orientation. However, the error of the 1D model is bounded. In lateral direction, the bikers are forced to stay on the track, which has a width of 6 m. Hence, they can not drive far away from the 1D line. Their yaw is also constrained to follow the 1D track approximately, because they have to take the track counter clockwise.

The 1D formulation of the track has the advantage that we can apply Theorem 1 from [5], which states that a 1D system is observable from gyrometer measurements alone if the rotation axis changes. At the entries and exits of the curves, the rotation axis changes. Hence, they can be detected.

Between the entries and exits of the curves dead reckoning is required. To reduce the drift, we can apply the forward velocity prior [8]. It makes the forward velocity observable. Hence, it can be estimated drift-free.

The initial guess is calculated by an Unscented Kalman Filter (UKF). Each state x_k consists of:

$$x_k = \begin{pmatrix} \lambda & \dot{\lambda} & Q_W^B & \vec{\omega}_B & \vec{v}_W & \vec{a}_W \end{pmatrix}^T \tag{11}$$

where λ is the position on the 1D line, $\dot{\lambda}$ the speed on the line and the rest is defined as in (2). The dynamic model is similar defined to (8) by:

$$g(x_k) = \begin{pmatrix} \lambda + \Delta t \cdot \dot{\lambda} \\ \dot{\lambda} \\ Q_W^B * \exp(\Delta t \cdot \vec{\omega}_B) \\ \vec{\omega}_B \\ \vec{v}_w + \Delta t \cdot \vec{a}_W \\ \vec{a}_W \end{pmatrix} \tag{12}$$

We formulated the main model by taking the difference of the measurement and a prediction function of the measurement as error. The same prediction function can be used in the measurement step of the UKF to apply the same information. In the case of prior knowledge, 0 is used as the target value. This is called a perfect measurement [18]. In this manner, (6) and (7) are used to incorporate the IMU measurements. Equation (9) is used to apply the forward velocity prior.

In the 1D Model, the bike follows the line only. Hence, we have to set $\dot{\lambda}$ to the norm of the velocity. This is done as a perfect measurement using the prediction function:

$$ld(x_k) = |\vec{v}_W| - \dot{\lambda} \tag{13}$$

Since the biker has to follow the track's direction, the angular rate has to be the direction change of the track approximately. In other words, the biker is likely to be in a curve if the gyrometer measures a nonzero angular rate. The prediction function is:

$$ar(x_k) = \vec{\omega}_B - R(\lambda) \cdot \dot{\lambda} \tag{14}$$

where $R(\lambda)$ is a function which returns the curvature of the 1D line at a given λ. This prior allows to observe the entry and exit points of the curves.

The UKF evaluates the probability distribution at different sigma points. If the covariance of the filter is underestimated, i.e. the UKF is too confident in the estimate, the distribution is evaluated poorly. Therefore, we apply high process noise, which allows the filter to correct implausible estimates. The high process noise models the vagueness of the 1D model.

The pseudo measurements are only useful in the curves of the track. At the straight parts, dead reckoning is performed implicitly. As a result the covariance rises quickly on the straight segments and is low when the biker drives a curve.

B. Missing IMU measurements

Approximately 5% of the IMU measurements are missing in the dataset for unknown reasons. In extreme cases, 50% of a 2 s interval are missing. Simply interpolating the missing measurements amplifies errors and is unsuitable for larger gaps. Therefore, we designed a solution that uses prior knowledge.

Neither the dynamic model, nor the prior knowledge require that the state has an input value (see Fig. 3). Thus, they are applicable for states with missing IMU data. Without an input measurement, the optimizer could choose arbitrary high acceleration and angular rate for the states. However, the measurements of the trials are bounded and lay in a certain range around 0. We incorporate this information by setting missing inputs to 0 and increasing the covariance of the measurement drastically to align the prior with the distribution of the dataset. This way, the optimizer chooses a realistic input that matches the heightmap and forward velocity prior.

C. Implementation details

The initial guess is smoothed with [19], which was modified for usage with the $\boxminus$ operator. This step backpropagates the information gained in the curves to the straight segments and improves the overall initial guess.

The main model has been implemented in ceres-solver, an extensive nonlinear least squares library [14]. It provides an automatic differentiation framework, which simplifies the use of nonlinear constraints, e.g. the prior knowledge. The Local Parameterization of ceres is used to adapt the rotation matrices without breaking them. Additionally, the rotation matrices are normalized every iteration.

Inputs, dynamic model and the prior knowledge are implemented as cost functions. The covariances for the Mahalanobis distances are shown in the Appendix.

To calculate the penalty for leaving the track, the closest point on the track is required. We approximate the closest point by taking the closest point on the x-y plane, i.e.:

$$h_k(x_k) \approx \vec{p}_W - \underset{\vec{c}_W \in Track}{\arg\min} \left| \left(\begin{smallmatrix} 1 & 0 & 0 \\ 0 & 1 & 0 \end{smallmatrix}\right) * (\vec{p}_W - \vec{c}_W) \right| \tag{15}$$

This enables us to precalculate the closest point for any x-y pair in a rectangle around the track and to store it in a 2D grid. Values between grid points are interpolated with a cubic spline using the algorithm of [20], which is already implemented in ceres. The smooth interpolation improves the gradient descent. Values outside the precalculated rectangle are extrapolated by taking the closest border point.

Since least square optimizers are prone to outliers, measurements exorbitantly outside the sensor range were removed from the dataset. They are treated as missing measurements.

IV. Dataset

We recorded the dataset[1] at the track of the Sixdays Bremen (see Fig. 1), an annual track cycling race. The track has a nominal length of 166.66 m and a width of 6 m. A heightmap (see Fig. 5) has been built based on the blueprints by [21].

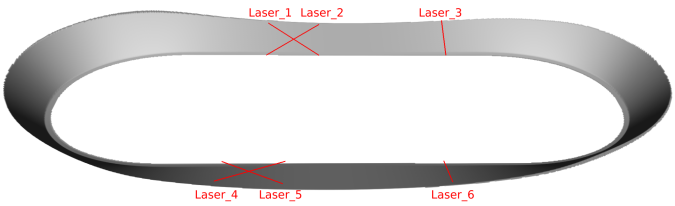

Fig. 5. Heightmap of the sixdays track. The red lines show the laser barriers.

We equipped the bike with four Xsens Awinda IMUs [22] at different links (see Fig. 2). The placement allows to estimate the joint angles of the bike using [23]. The crank IMU could be used to estimate the bikes velocity via wheel turn odometry. The sensors are connected wirelessly and measure at 100 Hz. They buffer the sensor data for 10 s during connection losses. Still, around 5% of the measurements are lost.

The bikes were also equipped with turn rate sensors to measure the velocity as a reference for the bikers only.

A tracking system that covers the complete track was not available. Thus, we used laser barriers to measure when the bikes pass a position.

We used six custom build laser barriers as ground truth reference. They trigger at 1024 Hz. The barriers are placed at the entries and exits of the curves (see Fig. 5). Two barriers are perpendicular to the track. The other 4 are arranged in two crosses. In each trial, one laser barrier failed to record data.

[1]Download at: http://www.informatik.uni-bremen.de/agebv/zavi

The moment when the bike's center line (see Fig. 2) passes the laser barrier is used as the ground truth measurement. It is calculated as the mean of the detected intervall in each round. This introduces a random error in the ground truth, which we guess around 5 ms. With a constant velocity assumption, the lateral position could be calculated at the crosses. With the known length of the bikes, the velocity could be estimated from the time the biker needs to pass each laser barrier.

The barrier clocks (2 ppm error) and the IMU base station (1ppm error) were synchronized before each trial. The accumulated time error after each trial is negligible.

The alignment of the barriers with the 3D model is imperfect. Thus, a bias of a few centimeters is introduced.

Two bikers participated in data recording using their own bikes. The dataset consists of two trials with Biker 1 and one with Biker 2. The bikers were tasked to drive the sequence:

1) Drive on the 166.66 m reference line
2) Stay in the 0.7 m corridor above the ref. line
3) Stay in the lower track half
4) Use the whole track
5) Repeat 2) with constant velocity
6) Repeat 3) with constant velocity
7) Drive as you wish

All tasks except 7) were executed for 10 rounds. This results in a driving distance of at least 10 km per trial and a driving time of approximately 20 min. The tasks could be used to test the use of prior knowledge with different strength, such as different corridor widths.

In addition, calibration motions were recorded for both bikes. These can be used to calibrate the position $\vec{t}_I$ and orientation Q_I^B of the IMUs with respect to the body frame.

V. Results

The trials are evaluated using the measurements of the main frame IMU. The laser barriers are only used as ground truth. The estimated trajectories stay on the track (see Fig. 6).

Since we do not have continuous ground truth position, we evaluate the error indirectly. We predict when the center line of the bike passes the laser barriers and compare the prediction with the measurement (see Fig. 6). TABLE I shows errror metrics. To transfer the time error into a position error, multiply it by the highest velocity of the trial ($\sim 12\,m/s$).

The estimator predicts passing the laser barrier with an average RMS of 0.096 s. The prediction error is higher than the error of the barriers. It does not increase over time, but

TABLE I

Mean error $\bar{e}$, mean absolute error $\overline{|e|}$, Root-Mean-Squared error RMS, max. error e_{max} and standard deviation σ of time errors in seconds. Trial 1 (orange), Trial 2 (green) and Trial 3 (yellow).

laser #	$\bar{e}$	$\overline{\|e\|}$	RMS	e_{max}	σ	$\bar{e}$	$\overline{\|e\|}$	RMS	e_{max}	σ	$\bar{e}$	$\overline{\|e\|}$	RMS	e_{max}	σ
1	-0.006	0.055	0.094	0.630	0.094	-0.016	0.066	0.085	0.372	0.083	-0.028	0.066	0.079	-0.173	0.074
2	-	-	-	-	-	0.056	0.096	0.121	-0.625	0.107	0.081	0.083	0.089	0.158	0.037
3	0.085	0.087	0.110	0.296	0.070	0.081	0.083	0.122	0.508	0.092	-	-	-	-	-
4	0.073	0.079	0.093	0.294	0.058	-	-	-	-	-	0.032	0.081	0.098	-0.309	0.093
5	0.075	0.075	0.097	0.386	0.061	0.098	0.102	0.172	1.010	0.141	0.030	0.044	0.063	0.280	0.056
6	0.039	0.047	0.061	0.221	0.047	0.024	0.055	0.072	-0.324	0.068	-0.011	0.056	0.081	-0.270	0.080

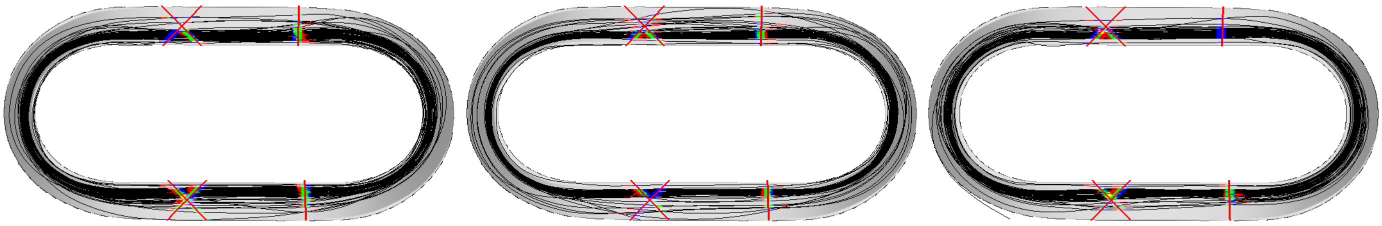

(a) Trajectory Trial 1 (b) Trajectory Trial 2 (c) Trajectory Trial 3

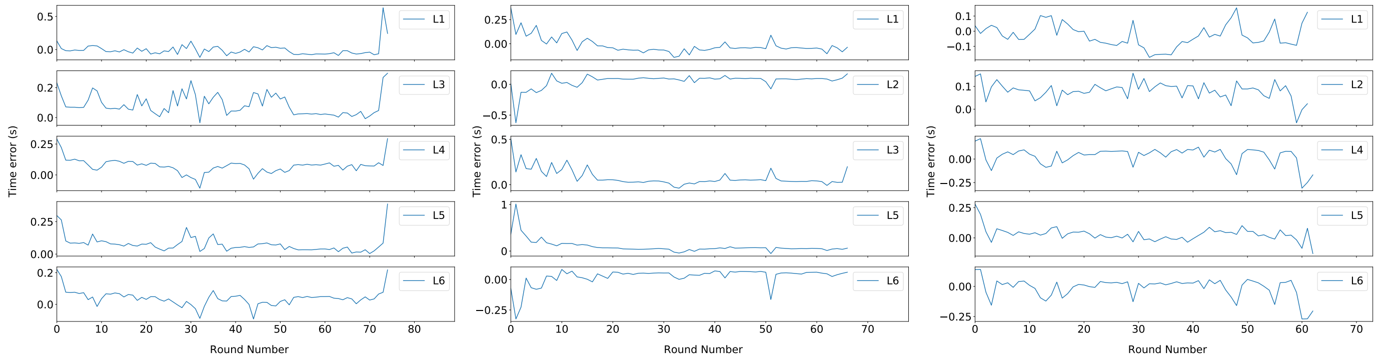

(d) Time error Trial 1 (e) Time error Trial 2 (f) Time error Trial 3

Fig. 6. (a-c) Trajectory of biker in all trials after 500, 500 and 250 iterations respectively. The lasers are shown as red lines. Blue color means that the estimator predicts that the bike passes a laser barrier. Red color means that a barrier measured that a bikes passes. Green color shows where prediction and measurement agree. (d-f) Time error between measured pass time and predicted pass time of the laser barriers.

it has a random component. Since it does not increase, the estimate error is drift-free.

High time errors occur often at the first and last rounds (see Fig. 6). Since we did not apply a start or end position constraint on the state estimate, the end and start point are less constrained than a point in the middle of the trial. Therefore, the error can be higher at those points. Also the bikes are slower at the the start and end (roll out), which increases the dead reckoning time between the curves.

In Trial 3, the end point is off the track. In Trial 2, it is almost off track. These are additional hints that the constraints are weaker at the start and end points.

The standard deviations are mostly lower than the RMS. Thus, the estimate is biased. To have a measure of the bias, the mean error is used. The highest mean error is 0.098 s. In certain cases, the bias is almost equal to the mean absolute error. Hence, it has a big impact on the quality of the estimate.

The bias of each laser barrier is variable over the trials. Thus, the bias is not purely systematic, e.g. caused by wrong alignment between heightmap and lasers. The biases are probably introduced by the prior knowledge. In [24], it was already discovered that a constrained estimator may be biased.

Overall, the estimates are surprisingly close to the ground truth data. The drift is corrected by the used prior knowledge. The average RMS of 0.096 s ($\sim$1.15 m) is low and comparable to the accuracy of pedestrian tracking systems without dedicated external hardware [1], [6]. The error has a few high peaks, which would affect an application. At the current state, the method can not compete in accuracy with off-the-shelf indoor GPS systems with +-2 cm error [25]. Nevertheless, we consider our results a successful tracking of the biker, which does not require external reference sensors.

A. Interpolated imu data

The missing IMU data is interpolated by the estimator. Most of the inserted values lay in a realistic range (see Fig. 7). In certain cases, the inserted values are unrealistically high. Probably, the prior knowledge was violated in these cases, for which reason the estimator used the vagueness of the missing measurements to correct the error.

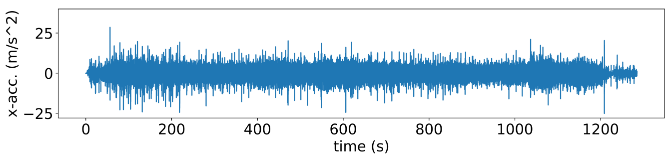

(a) Measured x-acceleration (IMU frame)

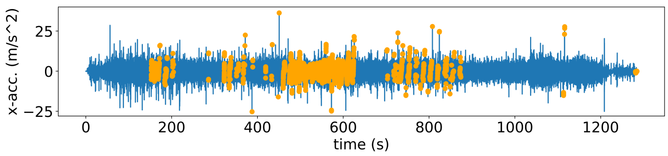

(b) Reconstructed x-acceleration (IMU frame)

Fig. 7. X-acceleration of Trial 1. Orange points have no valid IMU data.

B. Effect of knowledge

We want to investigate the influence of the used knowledges on the quality of the state estimate. The initial guess itself

TABLE II
TIME ERROR OF THE INITIAL GUESS (TRIAL 1)

laser #	$\overline{e}$	$\overline{\lvert e \rvert}$	RMS	e_{max}	σ
1	0.452	0.458	0.551	2.670	0.314
2	-	-	-	-	-
3	0.369	0.380	0.412	0.933	0.183
4	0.323	0.334	0.363	0.676	0.166
5	0.364	0.380	0.437	1.291	0.242
6	0.192	0.210	0.243	0.586	0.149

is already a good guess of the real trajectory. It is drift-free and has a time error of up to 2.670 s (see TABLE II). The maximum error is smaller than a half round, which means that all rounds are detected. The straights and curves of the track are matched to the track. With this initial guess, the least squares solver has to correct only local errors.

Using the forward velocity prior, we expect to have locally correct segments with a global pose drift. The estimated trajectory matches this expectation (See Fig. 8). The curves and the straights are clearly visible. However, the estimate leaves the track and has a false heading.

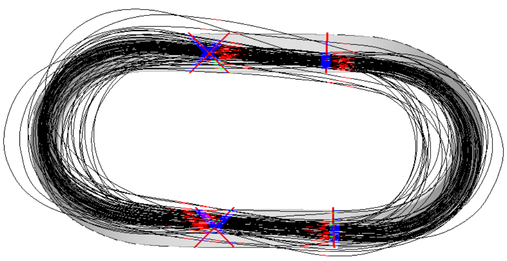

Fig. 8. Trajectory of Trial 1 without heightmap prior (100 iterations)

If only the heightmap prior is used, the estimate stays mainly on the track (see Fig. 9). The estimate does not drift. Again, this matches the expectation that the heightmap contains positional information. The RMS has decreased compared to the initial guess (see TABLE III). The estimate is similar to the estimate with both priors (see Fig. 6).

By making the forward speed observable, the forward velocity prior adds local correctness to the pose estimate. Only the starting pose of a segment is unknown if the prior is used. An INS without the prior would have local correctness as well, but without knowing the starting velocity of the segments. Hence, the segments would be deformed.

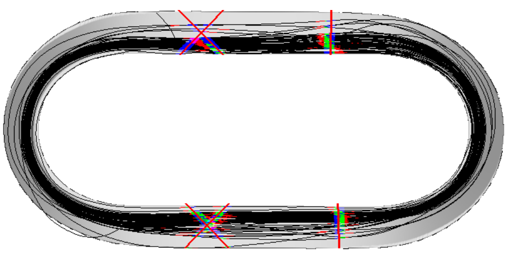

Fig. 9. Trajectory of Trial 1 without forward velocity prior (100 iterations)

TABLE III
TIME ERROR OF TRIAL 1 WITHOUT FORWARD VELOCITY PRIOR

laser #	$\overline{e}$	$\overline{\lvert e \rvert}$	RMS	e_{max}	σ
1	-0.094	0.128	0.157	0.600	0.125
2	-	-	-	-	-
3	-0.006	0.096	0.136	-0.557	0.135
4	-0.051	0.085	0.107	-0.309	0.094
5	0.011	0.094	0.219	1.651	0.219
6	-0.049	0.087	0.116	0.428	0.105

The heightmap prior adds global correctness and acts like an exteroceptive sensor. It matches the segments to a world pose implicitly, wherefore the drift is corrected. Since the IMU measurements provide local correctness alone, it can work without the forward velocity prior. However, the least squares solver may stuck in a local minima if it is initialized badly.

The combination of both priors yields the best results. This is not a surprise since state estimators generally get better if correct information is added.

VI. CONCLUSION AND FUTURE WORK

The pose of a track cycler can be estimated drift-free with an IMU as the only sensor, if it is combined with a heightmap of the track and the forward velocity prior. We have shown for three trials, each with more than 60 rounds, that the pose estimate does not drift. The estimator predicts passing laser barriers with an average RMS of 0.096 s, which is approximately 1.15 m over all trials. Thus, it is inferior to indoor positioning systems with external reference [25], but comparable to other IMU only systems [6].

An approximate model of the state space can be used to incorporate prior knowledge. For the initial guess, the track's surface is approximated as a 1D line. The initial guess is already a drift-free estimate of the trajectory.

We evaluated the influence of the used prior knowledges empirically. As expected from our observability analysis [5], the forward velocity prior yields local correctness of segments, whereas the heightmap prior yields global correctness.

Overall, the tracking accuracy is promising, but has outliers in particular at the start and end of the trial. It has been confirmed that a track cycler can be tracked drift-free with an IMU as the only sensor. Analysing the state observability through prior knowledge has led to this new, feasible application.

In future work, it has to be investigated how the accuracy of the state estimation can be improved. A dataset without missing data would be beneficial.

We used an state estimator that evaluates the complete trial data at once. This method is computationally expensive and not real-time capable. It has to be investigated if online methods, i.e. filters, can reach similar accuracy. We suggest using a Rao-Blackwellized PF [26], where segments derived with the forward velocity prior are used as dynamic update and the heightmap is used to weight the particles similar to the approaches in pedestrian dead reckoning [2].

Up to now, we argued that the pose of the biker is observable based on a theorem which is made for 1D systems [5].

Our results support the assumption. However, we want to generalize the theorem for 2D systems like the track cycling. With this, we want to deepen the insight into the paradigm of state observability through prior knowledge.

ACKNOWLEDGMENTS

We would like to thank Lukas Post for supporting the creation of the dataset, Peter von Maydell and Dennis Paul for participating as bikers and the organisers of the Sixdays Bremen for their permission to record the dataset.

APPENDIX

Covariances: Process noise applies on the dynamic model constraint (8). The $\vec{a}_I$ measurement noise consists of the sensor noise and additional noise which is caused by the transform from IMU acceleration to the body acceleration.

TABLE IV
COVARIANCES OF THE INITIAL GUESS

Process noise λ	$10\,m^2/s$
Process noise $\dot{\lambda}$	$0.1\,m^2/s^2/s$
Process noise Q_W^B	$0\,rad^2/s$
Process noise $\vec{\omega}_B$	$1\,rad^2/s^2/s$
Process noise $\vec{v}_W$	$0\,m^2/s^2/s$
Process noise $\vec{a}_W$	$100\,m^2/s^4/s$
$\vec{\omega}_I$ measurement noise (6)	$3.05 \cdot 10^{-6}\,rad^2/s^2$
$\vec{a}_I$ measurement noise (7)	$0.2004\,m^2/s^4$
Forward velocity prior (9)	$0.1\,m^2/s^2$
$\dot{\lambda}$ pseudo measurement noise (13)	$0.2\,m^2/s^2$
$\vec{\omega}_B$ pseudo measurement noise (14)	$0.5\,rad^2/s^2$

TABLE V
COVARIANCES OF THE MAIN MODEL

Process noise $\vec{p}_W$ in Σ_g	$0.1\,m^2/s$
Process noise $\vec{v}_W$ in Σ_g	$0.1\,m^2/s^2/s$
Process noise $\vec{a}_W$ in Σ_g	∞
Process noise Q_W^B in Σ_g	$0.1\,rad^2/s$
Process noise $\vec{\omega}_B$ in Σ_g	$0.1\,rad^2/s^2/s$
Process noise $\vec{\omega}'_B$ in Σ_g	∞
Process noise $\vec{b}_a$ in Σ_g	$8.28 \cdot 10^{-9} m^2/s^4/s$
Process noise $\vec{b}_g$ in Σ_g	$0.58 \cdot 10^{-9} rad^2/s^2/s$
$\vec{\omega}_I$ measurement noise (6) in Σ_{gy}	$3.05 \cdot 10^{-6}\,rad^2/s^2$
Missing angular rate noise (6) in Σ_{gy}	$1 rad^2/s^2$
$\vec{a}_I$ measurement noise (7) in Σ_{ac}	$0.2004\,m^2/s^4$
Missing acceleration noise (7) in Σ_{ac}	$400 m^2/s^2$
Forward velocity prior (9) in Σ_{fv}	$0.1\,m^2/s^2$
Heightmap prior (10) in Σ_h	$0.1\,m^2$

REFERENCES

[1] D. Lymberopoulos, J. Liu, X. Yang, R. R. Choudhury, V. Handziski, and S. Sen, "A realistic evaluation and comparison of indoor location technologies: Experiences and lessons learned," in *Proceedings of the 14th International Conference on Information Processing in Sensor Networks*, ser. IPSN '15. New York, NY, USA: ACM, 2015, pp. 178–189. [Online]. Available: http://doi.acm.org/10.1145/2737095.2737726

[2] R. Harle, "A survey of indoor inertial positioning systems for pedestrians." *IEEE Communications Surveys and Tutorials*, vol. 15, no. 3, pp. 1281–1293, 2013.

[3] S. Beauregard, Widyawan, and M. Klepal, "Indoor PDR performance enhancement using minimal map information and particle filters," in *2008 IEEE/ION Position, Location and Navigation Symposium*, 5 2008, pp. 141–147.

[4] O. Woodman and R. Harle, "Pedestrian localisation for indoor environments," in *Proceedings of the 10th International Conference on Ubiquitous Computing*, ser. UbiComp '08. New York, NY, USA: ACM, 2008, pp. 114–123. [Online]. Available: http://doi.acm.org/10.1145/1409635.1409651

[5] T. L. Koller, T. Laue, and U. Frese, "State observability through prior knowledge a conceptional paradigm in inertial sensing," in *Proceedings of the 16th International Conference on Informatics in Control, Automation and Robotics (ICINCO)*, 2019.

[6] B. Zhou, Q. Li, Q. Mao, W. Tu, and X. Zhang, "Activity sequence-based indoor pedestrian localization using smartphones," *IEEE Transactions on Human-Machine Systems*, vol. 45, no. 5, pp. 562–574, 2015.

[7] E. Foxlin, "Pedestrian tracking with shoe-mounted inertial sensors," *IEEE Computer Graphics and Applications*, vol. 25, no. 6, pp. 38–46, 11 2005.

[8] G. Dissanayake, S. Sukkarieh, E. Nebot, and H. Durrant-Whyte, "The aiding of a low-cost strapdown inertial measurement unit using vehicle model constraints for land vehicle applications," *IEEE transactions on robotics and automation*, vol. 17, no. 5, pp. 731–747, 2001.

[9] Y. Rothman, I. Klein, and S. Filin, "Analytical observability analysis of INS with vehicle constraints," *Navigation: Journal of The Institute of Navigation*, vol. 61, no. 3, pp. 227–236, 2014.

[10] L. Xu, Y. Liang, Q. Pan, Z. Duan, and G. Zhou, "A kinematic model of route-based target tracking: Direct discrete-time form," in *2016 19th International Conference on Information Fusion (FUSION)*, July 2016, pp. 225–231.

[11] G. Battistello, M. Ulmke, F. Papi, M. Podt, and Y. Boers, "Assessment of vessel route information use in bayesian non-linear filtering," in *2012 15th International Conference on Information Fusion*, July 2012, pp. 447–454.

[12] J. López-Araquistain, Ángel J. Jarama, J. A. Besada, G. de Miguel, and J. R. Casar, "A new approach to map-assisted bayesian tracking filtering," *Information Fusion*, vol. 45, pp. 79 – 95, 2019. [Online]. Available: http://www.sciencedirect.com/science/article/pii/S1566253517300933

[13] A. Dean, R. Martini, and S. Brennan, "Terrain-based road vehicle localisation using particle filters," *Vehicle System Dynamics*, vol. 49, no. 8, pp. 1209–1223, 2011. [Online]. Available: https://doi.org/10.1080/00423114.2010.493218

[14] S. Agarwal, K. Mierle, and Others, "Ceres Solver," http://ceres-solver.org.

[15] N. P. Craig and K. I. Norton, "Characteristics of track cycling," *Sports Medicine*, vol. 31, no. 7, pp. 457–468, Jun 2001. [Online]. Available: https://doi.org/10.2165/00007256-200131070-00001

[16] C. Hertzberg, R. Wagner, U. Frese, and L. Schröder, "Integrating generic sensor fusion algorithms with sound state representations through encapsulation of manifolds," *Information Fusion*, vol. 14, no. 1, pp. 57–77, 2013.

[17] M. Kok, J. D. Hol, and T. B. Schön, "Using inertial sensors for position and orientation estimation," *CoRR*, vol. abs/1704.06053, 2017. [Online]. Available: http://arxiv.org/abs/1704.06053

[18] G. Rasool, "Constrained state estimation-a review," *arXiv preprint arXiv:1807.03463*, 2018.

[19] S. Särkkä, "Unscented Rauch–Tung–Striebel Smoother," *IEEE Transactions on Automatic Control*, vol. 53, no. 3, pp. 845–849, April 2008.

[20] R. Keys, "Cubic convolution interpolation for digital image processing," *IEEE Transactions on Acoustics, Speech, and Signal Processing*, vol. 29, no. 6, pp. 1153–1160, December 1981.

[21] L. Post, "Positionsschätzung eines Bahnrennrades auf der Basis von Inertialsensordaten und Umgebungswissen," B.S. Thesis, University of Bremen, 2018.

[22] D. Roetenberg, H. Luinge, and P. Slycke, "Xsens MVN: Full 6DOF human motion tracking using miniature inertial sensors," *Xsens Motion Technol. BV Tech. Rep.*, vol. 3, 01 2009.

[23] F. Wenk, "Inertial motion capturing rigid body pose and posture estimation with inertial sensors," Ph.D. dissertation, University of Bremen, 2017.

[24] M. Podt, M. Bootsveld, Y. Boers, and F. Papi, "Exploiting imprecise constraints in particle filtering based target tracking," in *17th International Conference on Information Fusion (FUSION)*, July 2014, pp. 1–8.

[25] M. Robotics, "Marvelmind indoor GPS," https://marvelmind.com/.

[26] S. Thrun, W. Burgard, and D. Fox, *Probabilistic robotics*. MIT press, 2005.